PCCP

A Coarse-Grain Force Field Based on Quantum Mechanics (CGq FF) for Molecular Dynamics Simulation of Poly(Ethylene Glycol)-block-Poly(ε-Caprolactone) (PEG-b-PCL) Micelles

Journal:	*Physical Chemistry Chemical Physics*
Manuscript ID	CP-ART-08-2020-004364.R1
Article Type:	Paper
Date Submitted by the Author:	10-Sep-2020
Complete List of Authors:	Sadeghi, Maryam Sadat; Iran University of Science and Technology, Chemical, Petroleum and Gas Engineering; California Institute of Technology, Materials and Process Simulation Center Moghbeli, Mohammad Reza; Iran University of Science and Technology, School of Chemical, Petroleum and Gas Engineering Goddard, William; California Institute of Technology, Materials and Process Simulation Center

SCHOLARONE™
Manuscripts

A Coarse-Grain Force Field Based on Quantum Mechanics (CGq FF) for Molecular Dynamics Simulation of Poly(Ethylene Glycol)-block-Poly(ε-Caprolactone) (PEG-*b*-PCL) Micelles

Maryam S. Sadeghi,[†‡] M. R. Moghbeli,[1*†‡] William A. Goddard III[*‡]

[†‡] *Smart Polymers and Nanocomposites Research Group, School of Chemical Engineering, Iran University of Science and Technology, Tehran 16846–13114, Iran.*

[‡] *Materials and Process Simulation Center (MSC), California Institute of Technology, Pasadena, California 91125. USA*

1[*] Corresponding author email address: W. A. Goddard III (wag@caltech.edu), M. R. Moghbeli (mr_moghbeli@iust.ac.ir)
ORCID wag:0000-0003-0097-5716

Abstract

In order to provide the means to predict from molecular dynamics (MD) simulations the structures of copolymer-based micelles in solution, we developed coarse grain force field (CGq FF) parameters for poly(ethylene glycol) (PEG) and for poly(ε-caprolactone) (PCL). A key advance here is the use of quantum mechanics to train the parameters describing the non-bonded (NB) interactions between the CG beads. The functional forms are the same as the MARTINI CG FF so standard MD codes can be used. Our CGq FF describes well the experimentally observed properties for the polymer-air and polymer-water interfaces, indicating the accuracy of the NB interactions. The structural properties (density, radius of gyration (Rg), and end-to-end distance (h)) match both experiment and All Atom (AA) simulations. We illustrate the application of this CGq FF by following the formation of a spherical micelle from 250 chains of PEG_{23}-***b***-PCL_9 diblock copolymer, each block with molecular weight of 1000 Dalton, (10,500 beads, corresponding to 123,250 atoms) in a water box with 119,139 water beads (426,553 water molecules).

1. Introduction

Polymers form a complex class of substances in which the mechanical and physical properties arise from a broad range of length scales ranging from nanometers (monomers), polymer chains (with radii of gyration from 10-100 nanometers), to polymer networks (micrometer), to bulk materials (millimeter) with time scales ranging from nanoseconds to seconds/minutes/hours and even years [1,2]. Predicting the properties of such systems requires a hierarchy of methods starting with atomistic quantum mechanics (QM) and all atom (AA) force fields. In particular, we are interested in polymeric micelles comprised of a hydrophilic polymer block (forming the shell of the micelle), such as poly(ethylene glycol) (PEG), coupled with a hydrophobic polymer core, such as poly(ε-caprolactone) (PCL). An issue in providing a realistic description of such complex biological molecules and micelles is to capture the fundamental properties and conformations of the structures. This requires developing accurate force fields that describe the long range electrostatic and van der Waals (vdW) interactions. To make this practical we have developed coarse grain force field (CGq FF) parameters, in which each bead describes several atoms, for both PEG and PCL, including the junction in the copolymer.

Previous studies have parameterized PEG and PCL within the MARTINI CG scheme, as summarized below. The MARTINI FF is a thermodynamic based CG model useful for biological lipid membranes, proteins, carbohydrates, and fullerene molecules [3,4]. The MARTINI FF is parameterized to reproduce densities and free energies of partitioning between polar and apolar phases [5], but there are uncertainties in the parameters to describe the long range non-bonded (NB) interactions between the CG beads, where the NB parameters (van der Waals (vdW) and electrostatic) have not been validated against QM.

In 2009, Lee et al. followed the MARTINI parameterization approach to develop the first CG parameters for PEG melts and solutions. In their model the SNda MARTINI bead is taken to describe the PEG self-interaction and the interaction with water, with all the other interactions modeled using the SNa MARTINI bead. They validated their model by extracting structural properties of the polymer and comparing to AA simulations [6]. In a later study, they changed the SNa bead to SN0 and used the new parameters to reduce the excessive adsorption of PEO tails onto lipid head groups. This new model resulted in good predictions for structural properties with

various PEG molecular weights, however, it exhibited instabilities due to bad dihedral potentials for the polymer backbone [7].

Rossi et al. refined the Lee model by introducing of new valence parameters to reduce the instability of the Lee model due to the dihedral potentials in the backbone of the polymer. They introduced a new bead type and torsion potential function for PEG and PEG alkyl ether systems, allowing them to use larger time steps of 20-25 fs [8]. In another study they provided a MARTINI-based CG model for polyethylene and polypropylene melts [9].

Nawaz et al. used the existing non-bonded parameters of standard MARTINI for Pluronics, a class of synthetic block copolymers, and derived the bonded parameters from single chain properties. Their model does not show good thermodynamic transferability for PEO homopolymer especially in water [10].

Taddese et al, developed a new CG model based on the solvation free energy of monomers in different solvents and proposed a simple method to select the non-bonded parameters to reproduce the partition coefficients. However, their model suffers from a transferability problem for larger molecular weights [11].

In 2018 Grunewald et al. parameterized a new CG model for PEG based on the energies for transfer of the shortest PEO oligomer (dimethoxyethane, PEO dimer) from water to solvents of various polarities. They proposed a new more hydrophobic bead for PEO that reproduced very well the structural properties of lipid layers containing PEGylated layers and PS-PEO block copolymers. However, their model failed to reproduce the phase behavior of high molecular weight PEO in water, which is a good solvent for PEO [12].

Choi et al. developed a MARTINI model for solvated PEG using water with a large multipole. The Choi FF removes the artifact of ring-like conformations seen in short PEG chains within MARTINI scheme [13].

Prasitnok et al. used the iterative Boltzmann inversion (IBI) method to develop a MARTINI based CG model for PEG that proved to be transferable to PEG chains at the water/air interface [14]. The Choi and Prasitnok models employ a water bead representing 3 water molecules that is different than the MARTINI P4 bead, consisting of 4 water molecules.

Very few studies have focused on parameterization of PCL. Raman et al. developed a CG model for PCL in which the non-bonded interactions were based on the existing MARTINI bead types while the bonded interactions were mapped from an OPLS-UA/AA simulation of PCL. They studied the self-assembly of methoxy-poly(ethylene glycol)-block-poly(ε-caprolactone) (MePEG-b-PCL) linear diblock copolymers, using the Lee model for PEG. Their model reproduced the structural and dynamic properties of PCL homopolymers, however, it underestimated the size of the resulting micelles by a factor of 1.48 [15].

Loverde et al. used molecular dynamics (MD) simulations to build a rational CG (rCG) model for PCL. Taking the Shinoda parameters for PEG [16], they built a CG model for diblock copolymers of poly(ethylene glycol)-block-poly(ε-caprolactone) (PEG-***b***-PCL), that they used to study the shape-dependent effects in delivery of the widely used anti-cancer drug, Taxol by block copolymer micelles [17].

None of these studies focused on the crystalline or semi-crystalline phases for polymers such as PEG. It is important to note that the semi-crystalline polymers such as PEG and PEO have a multiphase character with amorphous and crystalline regions at various temperatures [18]. In particular, we consider the crystalline phases of semi-crystalline polymers important because they provide valuable information on the NB interactions of the systems. Therefore, we propose and apply here the use of quantum mechanics to train the parameters describing the NB interactions between the CG beads, denoted as CGq FF. The functional forms of CGq FF are the same as the MARTINI CG FF so that standard molecular dynamic (MD) codes can be used.

The New Non-bonded Interaction Parameters

To obtain the NB parameters for these polymers we build on the recent advance by Naserifar et.al, who showed that the PBE-D3 level of DFT describes the equation of state for molecular crystals accurately up to 100's of GPa [19]. This uses the D3 Grimme empirical vdW function with parameters optimized by Becke and Johnson. Thus, we constructed polymer crystals of PEG and PCL and carried out PBE-D3 level DFT calculations to optimize the CG NB parameters to reproduce the QM lattice spacings and cohesive energies.

We validate the CGq FF for each polymer by showing that:

1. It leads to polymer radius of gyration and end-to-end distance that agree with experiment and atomistic simulations for a broad range of molecular weights,
2. The interactions between EO (ether) sites of PEG and CL sites (CH2-CH2-CH2-CH2 site and CH2-C-O-O site) for PCL lead to intra-molecular radial distribution functions (RDF) between the center of mass of two adjacent repeating units that agree with atomistic simulation and,
3. It reproduces the polymer-air and polymer-water interfacial properties.

We illustrate the application of the CGq FF by following the self-assembly of diblock copolymers based on PEG-***b***-PCL in aqueous solution and analyzing the structural features of the formed micelle.

2. Methods and Models

2.1. Atomistic Simulations

PEG System Single Chain in Water: Atomistic simulations were performed with the GROMACS 5.1.4 package, using four different FF parameterizations commonly applied to simulation of biological molecules: AA CHARMM36, AA CHARMM27, OPLS-AA and UA Gromos54-a7 FF.

The PEG system involves a single chain starting from the all-trans extended conformation, consisting of 9-mers, HO-(CH2-CH2-O)$_9$-H (PEG_9) solvated in a box of 55.7 Å/side using ~5,740 water molecules; (for CHARMM36 and CHARMM27 we used the TIP3P water model while for Gromos54-a7 and OPLS-AA FFs we used the SPCE water model).

All simulations were initialized using energy minimization to relax any unphysical atomic overlaps. The steepest descents (SD) algorithm was used for all relaxations unless otherwise stated. The SD was terminated once the maximum force on any one atom was less than 500 kJ/mol.nm. Then the systems were equilibrated using the canonical NVT ensemble (constant particle number - N, constant volume - V and constant temperature - T) for 1 ns, followed by another equilibration in the isothermal-isobaric NPT ensemble (constant particle number - N, constant volume - V and constant pressure - P) for 10 ns. Thereafter, this system was subjected to a 100 ns MD using the NPT ensemble.

The equations of motions were integrated using the leap-frog integrator with a 2 fs time step. Neighbor lists were updated every 10 steps and coordinates were saved every 2 ps. The temperature

and pressure were maintained at 300 K and 1 bar using a modified Berendsen thermostat (1ps damping constant) and Parrinello-Rahman barostat (10 ps damping constant). Long range electrostatic interactions were treated with the particle mesh Ewald method using a cutoff of 10 Å. The NB (Lennard-Jones (LJ)) interactions were shifted to zero at 10 Å using the Tapir smoothing function. The all-trans extended conformation of PEG_9 transformed to a random coil arrangement during the production run.

PCL System Single Chain in Water: The same atomistic simulation protocols were used for the PCL system, however in this case we used three different FF parameterizations: AA CHARMM27, OPLS-AA and UA Gromos54-a7 FF.

The PCL system involves a single chain starting from an all-trans extended conformation, consisting of 10-mers, HO-(CH2-CH2-CH2-CH2-CH2-COO)$_{10}$-OH (PCL_{10}) solvated in a box of 90.6 Å/side with ~25,700 water molecules; (for AA CHARMM27 FF we used the parameters of the TIP3P water model while for UA Gromos54-a7 and AA OPLS/CM1A FFs, SPCE water model was used).

2.2. CG Simulations

Single Chain in Water: The CG simulations used the GROMACS 5.1.4 package with the MARTINI FF developed by Marrink et al. [5]. The CG equations of motions were integrated using a time step of 10 fs. A NB cutoff of 12 Å was set for LJ and electrostatic interactions. The LJ potential was shifted to zero between 9 and 12 Å, while the coulomb potential was smoothly shifted to zero between 0 and 12 Å. The velocity rescale (V-rescale) thermostat was used with a coupling constant of 1 ps to maintain the temperature at 300 K while the pressure was controlled with the Parrinello-Rahman barostat using a coupling constant of 12 ps. The CG system was relaxed using steepest descents, then equilibrated for 10 ns using the NPT ensemble and then subjected to 100 ns MD in the NPT ensemble.

Mapping Schemes: The final AA trajectories of PEG_9 and PCL_{10} were mapped to the CG structure through the mapping matrix MRI (mapping AA coordinates r^n to CG coordinates R^N). Figure 1 shows the mapping of the atomistic structures to the CG structure for each PEG and PCL homopolymers and the PEG-***b***-PCL diblock copolymer.

PEG System: each CH2-O-CH2 unit in the PEG_9 backbone was grouped into one CG bead (new bead defined as Sd1) leading to a 3 to 1 mapping, while the HO-CH2 terminal groups were parameterized separately, using a 2 to 1 mapping (MARTINI SP2 bead). The CG-PEG structure was placed in a box of water with 57.2 Å/side, corresponding to the AA simulation (~1,600 MARTINI water molecules)

PCL System: For PCL, we defined four different beads to map the atomistic PCL_{10} structure to the CG structure. The terminal HO-CH2 and HO-CO-CH2 groups are mapped to the SP2 and SNa MARTINI standard beads, while the backbone monomer was partitioned into two new beads: the CH2-CH2-CH2-CH2 group is mapped to bead C0 and the CH2-C-O-O group is mapped to bead N1, leading to a 4 to 1 mapping for both cases. The CG-PCL structure was placed in a box of water with 90.6 Å/side with ~6,500 MARTINI water beads, corresponding to the AA simulation (each MARTINI water bead consists of 4 water molecules).

Water System: We used the CG MARTINI model for the water molecules. We tested that this model reproduces the experimental surface tension of water (detailed information provided in SI).

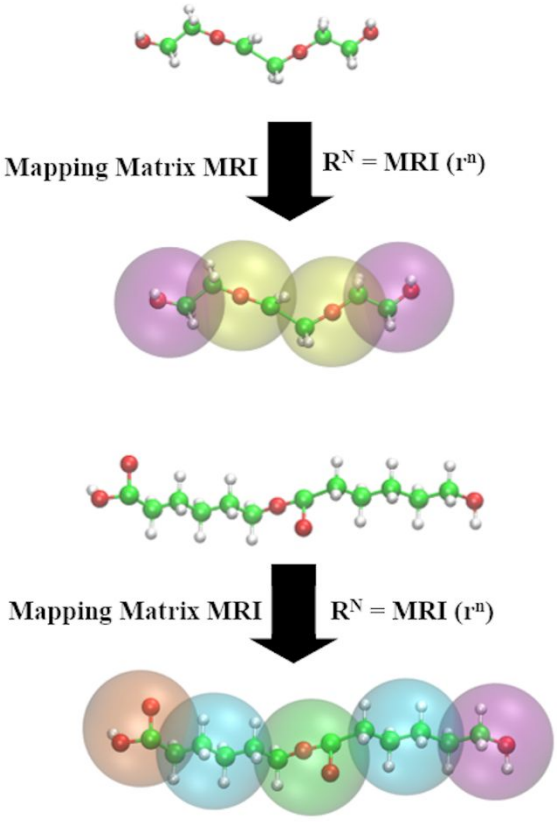

Figure 1. Illustration for mapping the All-Atom (AA) representation to the Coarse-Grained (CG) representation through the mapping matrix MRI (mapping AA coordinates r^n to CG coordinates R^N). Top: tetraethylene glycol (TeEG): AA: C- green, O- red, H- white. CG: SP2- purple, Sd1- yellow; Bottom: di(ε-caprolactone) (DiCL): AA: C- green, O- red, H- white. CG: SNa- orange, C0- blue, N1- lime, SP2- purple.

2.3. QM Calculations

The QM calculations were carried out using the Vienna Ab initio Simulation Package (VASP) [20-23]. The QM cohesive calculations were performed for the experimental crystalline structures of PEG and PCL, retrieved from the Cambridge Structural Database–CSD (Cambridge, UK) [24].

PEG System: The unit cell of the crystalline PEG is monoclinic with parameters $a = 8.05\text{Å}, b = 13.04\text{Å}, c(fiberaxis) = 19.48\text{Å}, \beta = 125.4°$, and the space group P21/a-C2h. The polymer chain is $(\text{-(CH2)}_\text{m}\text{-O-})_\text{n}$. The volume of the unit cell is 1666.82Å^3 and the density of the system is $1.229 g.cm^{-3}$ (Figure 2.a). From the positions of atoms in the first chain (x,y,z) and by space group operations, the positions of the 3 remaining symmetry-related chain images are obtained, xyz (first chain), -x-y-z (second chain), 0.5-x0.5+y-z (third chain), 0.5+x0.5-yz (fourth chain).

PCL System: The unit cell of the crystalline PCL is orthorhombic with dimensions $a = 7.496\text{Å}, b = 4.974\text{Å}, c(fiberaxis) = 17.297\text{Å}$, and the space group P212121. The polymer chain is $(\text{-CH2-CH2-CH2-CH2-CH2-COO-})_\text{n}$. The volume of the unit cell is 634.27Å^3 and the density of the system is 1.146 $g.cm^{-3}$ The unit cell contains two chains with opposite orientation (up and down), see Figure 2.b.

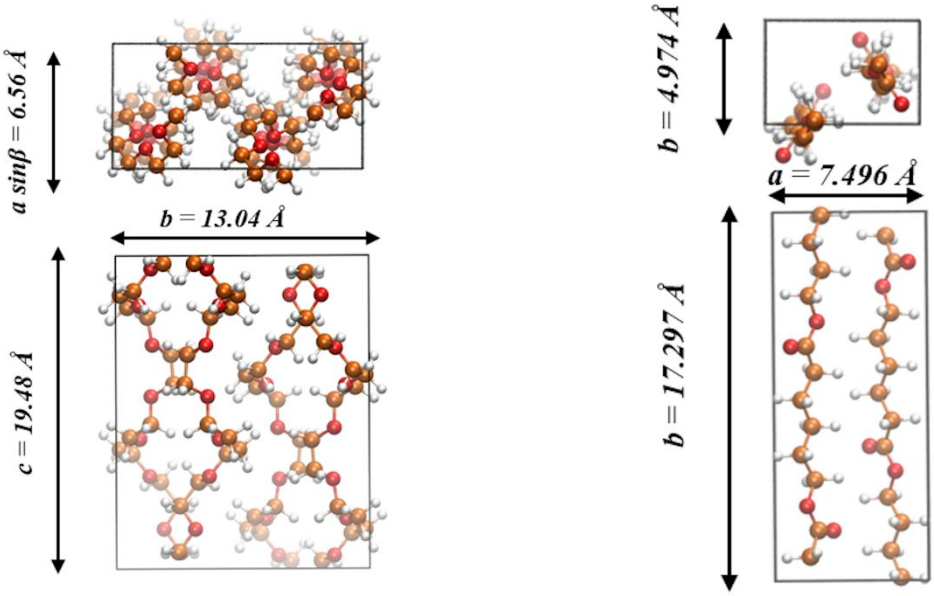

(a) **(b)**

Figure 2. (a) Crystalline structure of PEG, top: along the chain axis - ab plane and bottom: perpendicular to chain axis - bc plane. **(b)** Crystalline structure of PCL, top: along the chain axis - ab plane and bottom: perpendicular to chain axis ac - plane. Color code: C- orange, O- red, H- white.

QM Calculation Protocol: We used the PBE flavor of GGA DFT including the corrections for the vdW interactions using the Grimme D3 method with Becke-Johnson parameters [25]. The Gamma Centered Monkhorst-Pack Grid was applied with symmetry leading to a kmesh of 18 k points and the initial charge density was generated from the superposition of atomic charges. We used conjugate gradient minimization to optimize the atom positions and periodic cell parameters until the forces converged to 0.018 eV/A., The planewave cutoff energy was set to 600 eV and the break condition for the ionic relaxation loop was 10^{-3} and the global break condition for the electronic SC-loop was 10^{-4}.

3. Results and Discussion

3.1. Development of the New QM based Coarse Grain Force Field (CGq FF) Parameters

We derived our new CGq FF parameters by setting the different potential contributions in the order of their relative strengths, i.e. Ustretch → Ubend → Unon-bonded → Udihedral, where Ustretch, Ubend and Udihedral are the covalent contributions of the potential energy including the bond,

angle and dihedral terms and Unon-bonded is the noncovalent contribution, including the electrostatic and van der Waals interactions.

First, we fit the derived valence CG parameters of a single short chain of each homopolymer at high dilution in water to the distribution functions from the atomistic FF. Then to obtain the NB parameters for these polymers we build on the recent advance by Naserifar et.al, who showed that the PBE-D3 level of DFT describes the equation of state for molecular crystals accurately up to 100's of GPa. [19]. To do this we constructed polymer crystals of PEG and PCL and carried out PBE-D3 calculations to optimize the CG NB parameters to reproduce the QM lattice spacings, and cohesive energies, we denote this as the CGq FF.

3.2. Potential Energy Function

The functional form of the MARTINI potential energy consists of bonds, angles, Lennard-Jones (LJ) non-bonded, and electrostatic terms according to Equation 1:

$$V = \sum\frac{1}{2}K_{bond}(b - b_{bond})^2 + \sum\frac{1}{2}K_{angle}\{cos(\theta) - cos(\theta_0)\}^2 + \sum_{i=1}^{m}K_{\phi,i}(1 + cos(n_i\phi - \phi_i)) + \sum 4\epsilon_{ij}\left[\left(\frac{\sigma_{ij}}{r}\right)^{12} - \left(\frac{\sigma_{ij}}{r}\right)^{6}\right] + \sum\frac{q_iq_j}{4\pi\epsilon_0\epsilon_r r} \quad (1)$$

where K_{bond} is the bond force constant, b_{bond} is the equilibrium distance, K_{angle} is the angle force constant, θ_0 is the equilibrium bond angle, $K_{\phi,i}$ is the dihedral force constant, and n_i and ϕ_i are the multiplicities and offsets of the m individual dihedral terms . Here σ_{ij} is the inner wall point of the NB potential and ϵ_{ij} is the well depth at the minimum of the NB potential. Charged groups hold a full charge q_i, q_j and interact thru a shifted Coulombic potential energy function, with relative dielectric constant ϵ_r = 15 for explicit screening [5]. We do not use the charges q_i and q_j in our CGq FF model.

Some MARTINI models employ a dihedral potential along the backbone, but these have stability problems when one of the angles approaches 180 deg [26]. To avoid such instabilities in our simulations, we used the restricted bending potential, developed by Bulacu and co-workers (Equation 2), together with the cosine harmonic for PEG.

$$V_{angle} = \frac{1}{2}K_{angle}\frac{(cos\theta - cos\theta_0)^2}{sin^2\theta} \quad (2)$$

3.2.1. Derivation of Valence CG Parameters

The valence CG parameters were derived by mapping the AA model to the CG model and reproducing the distribution functions for AA MD of each polymer. Among the four tested AA and UA FFs, we found that AA-CHARMM36 and AA-OPLS/CM1A FF parameters provided the most accurate description of the structural properties of the short PEG_9 and PCL_{10} homopolymers (details are provided in SI). Therefore, the valence distribution functions of these two FFs were taken as target distributions to calculate the valence parameters of the CG-PEG and CG-PCL potential functions.

3.2.2. Derivation of QM based NB CG Parameters

The QM cohesive energy and density of the crystalline structure was used as the reference point to fit the CG NB potential parameters for each homopolymer. The cell parameters and the bond and angle parameters of the crystal was optimized at the PBE-D3 level. The QM cohesive energy was calculated by comparing the total NB energy (TE) for the optimized structure to the structures in which each fixed chain is moved to a large cell with cell parameters of $a,b = 52$Å. Then for the CG structure we optimized the LJ NB parameters to match the QM density and total NB energy (TE). The calculated NB cohesive energies and densities for the QM and CG structures are compared in Table 3 and 4.

3.2.3. CGq FF Parameters

The Lennard-Jones (LJ) σ_{ij} parameter for MARTINI beads representing 4 heavy atoms is 4.7 Å, while for smaller beads used with a 3 to 1 mapping this parameter is scaled to 4.3 Å. Instead, our new approach optimizes the NB parameters to fit QM.

PEG System: To characterize PEG we defined a new bead Sd1, with LJ parameters of ϵ_{ij}=3.4 kJ.mol^{-1} and σ_{ij}= 4.3 Å representing the core beads (section 3.2). The terminal beads are suitably represented by the MARTINI SP2 bead type. The final parameters for our CG-PEG potential energy function is given in Table 1. This leads to a calculated cohesive energy of –5.663 kcal.mol^{-1} compared to the QM value of -5.649 kcal.mol^{-1} and to a density of 1.280 compared to 1.311 for QM.

Table 1. CGq FF Parameters for PEG

	Valence Parameters			Non-bonded (NB) Parameters
atom (bead)	Bond	Angle	Dihedral	LJ (6-12)

	Simple Harmonic (* 1, 2)		Cosine Harmonic (* 2, 2) and Restricted Bending (* 10, 2)		Periodic Cosine (* 1, 4)			
	K_{bond} $(KJ.mol^{-1}.nm^{-2})$	b_{bond}(Å)	K_{angle} $(KJ.mol^{-1})$	$\theta_0(deg)$	$K_{\phi,i}$ $(KJ.mol^{-1})$	$\phi_i(deg)$	ϵ_{ij} $(KJ.mol^{-1})$	σ_{ij}(Å)
$SP2-Sd1$	10000.000	2.850	-	-	-	-	-	-
$Sd1-Sd1$	12000.000	3.250	-	-	-	-	-	-
$SP2-Sd1-Sd1$	-	-	76.046	135.00	-	-	-	-
$Sd1-Sd1-Sd1$	-	-	45.000	132.5	-	-	-	-
$Sd1-Sd1-Sd1$	-	-	5.000	132.5	-	-	-	-
$Sd1-Sd1-Sd1-Sd1$	-	-	-	-	1.96, 0.18, 0.33, 0.12	180, 0, 0, 0	-	-
$Sd1-Sd1$	-	-	-	-	-	-	3.4	4.3
$W-W**$	-	-	-	-	-	-	5.0	4.7

*** The function type and number of parameters with the GROMACS definition**.

*** * MARTINI parameters were taken for water beads (W-W) [5].**

PCL System: For PCL, we defined two new beads (section 3.2):

- C0, intermediate with LJ parameters of ϵ_{ij}=2.25 kJ.mol^{-1} and σ_{ij}= 4.65 Å and
- N1, semi-attractive with LJ parameters of ϵ_{ij}=3.65 kJ.mol^{-1} and σ_{ij}= 4.65 Å representing the core beads,

The terminal beads are represented by the MARTINI SP2 and SNa bead types. The final parameters for our CG-PCL potential energy function are given in Table 2. This leads to a calculated cohesive energy of –14.492 KCal.mol^{-1} compared to the QM value of -14.895 Kcal.mol^{-1} and to a density of 1.288 compared to 1.289 for QM.

Table 2. CGq FF Parameters for PCL

atom (bead)	Valence Parameters						Non-bonded (NB) Parameters	
	Bond		Angle		Dihedral		LJ (6-12)	
	Simple Harmonic (* 1, 2)		Cosine Harmonic (* 2, 2)		Periodic Cosine (* 1, 1)			
	K_{bond} $(KJ.mol^{-1}.nm^{-2})$	b_{bond}(Å)	K_{angle} $(KJ.mol^{-1})$	$\theta_0(deg)$	$K_{\phi,i}$ $(KJ.mol^{-1})$	$\phi_i(deg)$	ϵ_{ij} $(KJ.mol^{-1})$	σ_{ij}(Å)
$SNa-C0$	3800.000	3.500	-	-	-	-	-	-
$C0-N1$	4000.000	3.800	-	-	-	-	-	-
$C0-SP2$	3800.000	3.500	-	-	-	-	-	-
$SNa-C0-N1$	-	-			-	-	-	-
$SNa-C0-N1$	-	-	40.000	140.0	-	-	-	-
$C0-N1-C0$	-	-	40.000	110.0	-	-	-	-
$N1-C0-N1$	-	-	40.000	130.0	-	-	-	-
$N1-C0-SP2$	-	-	40.000	140.0	-	-	-	-
$C0-N1-C0-N1$	-	-	-	-	-3.000	0.231	-	-
$N1-C0-N1-C0$	-	-	-	-	-3.000	-5.729	-	-
$C0-C0$	-	-	-	-	-	-	3.20	4.65
$N1-N1$	-	-	-	-	-	-	3.65	4.65

$W-W^{**}$	-	-	-	-	-	-	5.0	4.7

*** The function type and number of parameters with the GROMACS definition**.

*** * MARTINI parameters were taken for water beads (W-W) [5].**

Crystal Density: We fitted the NB parameters to match the QM minimized crystal structures. To examine how well the CGq FF describes the changes in density and energy with temperature, we calculated the density of the CG crystal structure for each homopolymer after a short (50 ps) NVT simulation followed by a 2 ns NPT calculation at 300 K. The averaged cell parameters and density of the CG crystalline structure is compared with the experimental and QM structures in Tables 3 and 4.

Table 3. Cell Parameters, Density (ρ) and Cohesive Energy (COE) of the Crystalline PEG Structure at 300K

Crystal Parameters	a (Å)	b (Å)	c (Å)	β (deg)	$Volume$ ($Å^3$)	ρ ($g.cm^{-3}$)	T (K)	COE/monomer ($KJ.mol^{-1}$)
Experimental Structure *	8.050	13.040	19.480	125.400	1666.820	1.229	300	-
CG Structure [1]	8.399	13.419	17.132	103.816	1875.178	1.126	300	-
QM Structure [2]	7.959	12.716	19.711	126.897	1595.280	1.280	0	-5.649
CG [3]	7.959	12.716	19.711	126.897	1595.280	1.311	0	-5.663

***Experimental crystal parameters retrieved from [24].**
[1]: After dynamics, 300K; [2]:after minimization, 0K; [3]:after minimization, 0K.

Table 4. Cell Parameters, Density (ρ) and Cohesive Energy (COE) of the Crystalline PCL Structure at 300K

Crystal Parameters	a (Å)	b (Å)	c (Å)	β (deg)	$Volume$ ($Å^3$)	ρ ($g.cm^{-3}$)	T (K)	COE/monomer ($KJ.mol^{-1}$)
Experimental Structure *	7.496	4.974	17.297	90.000	634.270	1.195	300	-
CG Structure [1]	7.391	4.926	17.195	90.000	626.037	1.212	300	-
QM Structure [2]	7.144	4.799	17.168	90.000	588.589	1.288	0	-14.895
CG [3]	7.144	4.799	17.168	90.000	588.589	1.289	0	-14.492

***Experimental crystal parameters retrieved from [24].**
[1]: After dynamics, 300K; [2]:after minimization, 0K; [3]:after minimization, 0K.

3.3. Validating the CGq FF

3.3.1. Structural Properties

PEG System: We predicted the single chain conformations of CG-PEG in water at 300K for various lengths (9, 27, 36, 44, 67, 76, 90, 112, 135). Our calculated radius of gyration vs chain length is compared in Figures 3.a and 3.b with the AA-CHARMM36 FF (carried out in this work), as well as available experimental data, and previous computations. These show very good agreement between our results and available data.

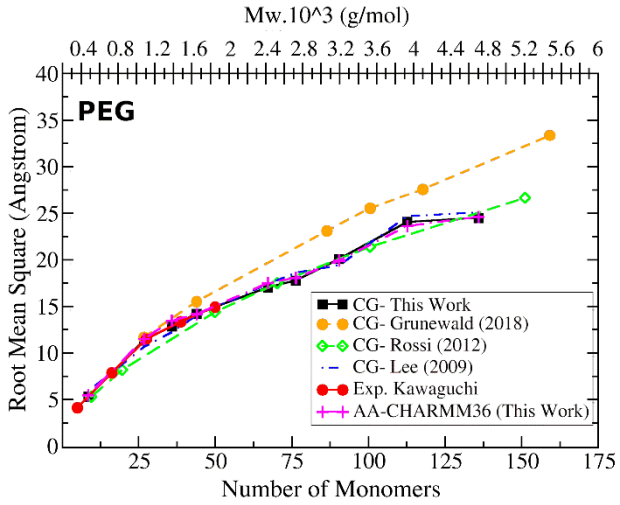
Mw.10^3 (g/mol)
0.4 0.8 1.2 1.6 2 2.4 2.8 3.2 3.6 4 4.4 4.8 5.2 5.6 6
PEG
Root Mean Square (Angstrom)
Number of Monomers
CG- This Work
CG- Grunewald (2018)
CG- Rossi (2012)
CG- Lee (2009)
Exp. Kawaguchi
AA-CHARMM36 (This Work)

(a)

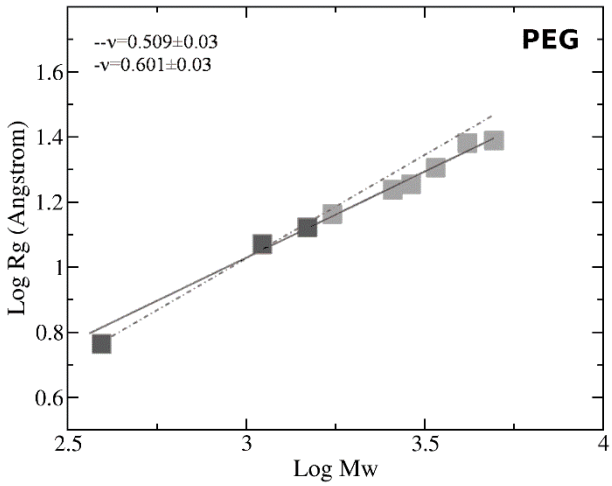
--ν=0.509±0.03
-ν=0.601±0.03
PEG
Log Rg (Angstrom)
Log Mw

(b)

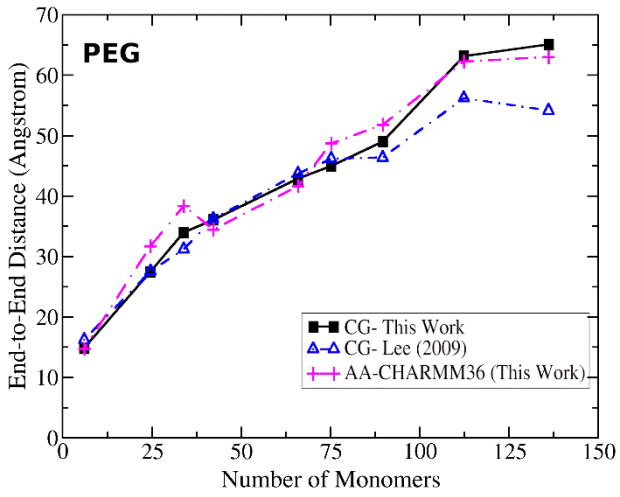

(c)

Figure 3. (a) The dependence of Rg on chain length for single chains of PEG in Water. Experimental data (red dots) are extrapolations to the small chain lengths from Kawaguchi et al. [27]. All simulations agree well with experiment except Grunewald (orange dots). **(b)** log Rg versus log Mw from simulations of CG-PEG_9-PEG_{135} for two regions, dashed line: 400<Mw<1648 and solid line: 1648<Mw<6972. **(c)** The dependence of End-to-End distance on chain length for single chains of PEG in Water.

Figure 3.b shows the transition from ideal to real chain behavior. We see a shift of the ν coefficient in $R_g \propto M_w^{\nu}$ from 0.509 to 0.601, which is within the statistical uncertainty of the experimental value: 0.583. The end-to-end distances of our CG-PEG systems (black squares) also compare well to the AA-CHARMM36 FF (purple pluses) in Figure 3.c.

PCL System: Single chains of CG-PCL with various lengths (10, 20, 30, 50, 75) were simulated in water at 300K. We compare the conformational properties for our CG systems with the AA-OPLS/ FF (carried out in other studies) and with previous CG computational data in Figures 4.a and 4.b. Our CG structural properties (Rg and end-to-end distance) agree with the AA- OPLS predictions from Di Pasquale.

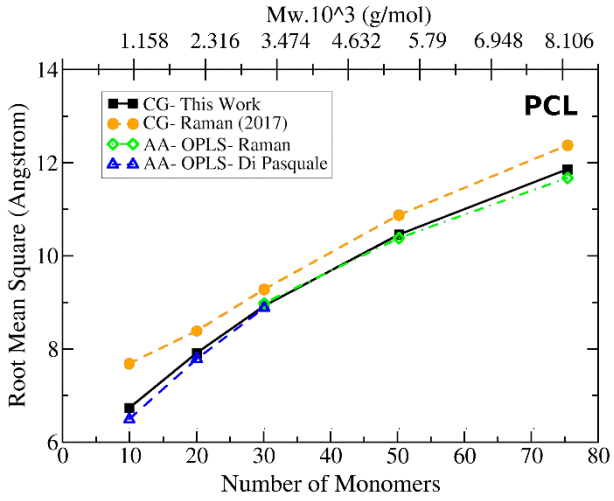

(a)

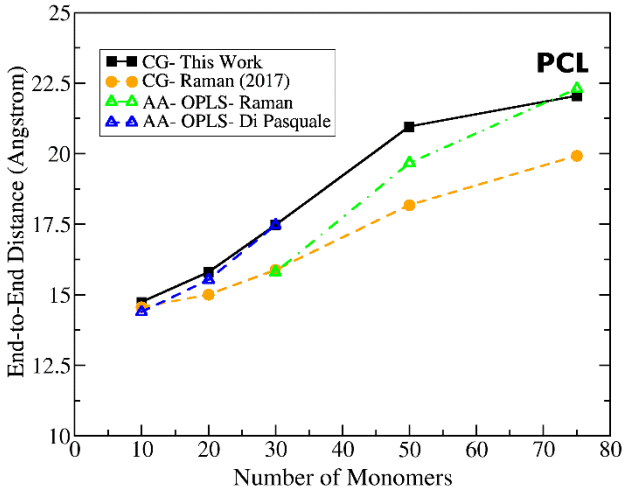

(b)

Figure 4. (a) The dependence of Rg on chain length for different single chains of PCL in Water. **(b)** The dependence of End-to-End on chain length for different single chains of PCL in Water.

3.3.2. Intra-Molecular Radial Distribution Function (RDF) The RDF is defined as [28]:

$$RDF(r) = \left(\frac{1}{4}\pi\rho r^2\right)\frac{dN(r)}{dr} \quad (3)$$

where ρ is the number density, r is the interatomic distance between the center of mass of the particles and N is the number of beads or central atoms within the distance r of the center of mass of the particles.

PEG System: Figure 5 compares the AA and CG intra-molecular Radial Distribution Functions (RDF) between two adjacent core beads (Sd1-Sd1) in the CG-PEG_9 structure and two adjacent ether oxygen sites (EO) in the AA structure.

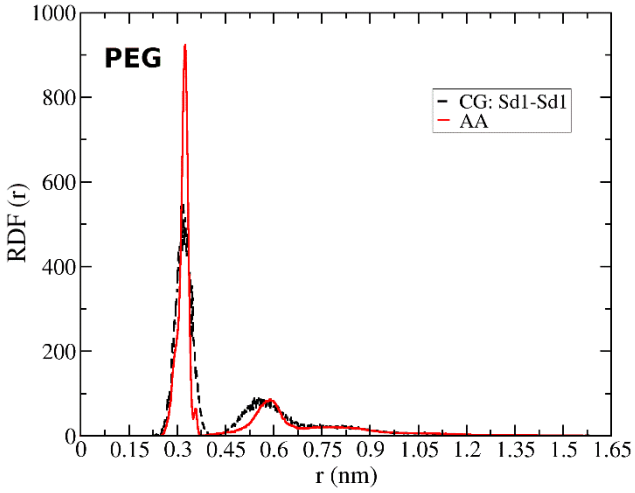

Figure 5. Radial distribution functions for Sd1-Sd1 sites from CG (dashed line, black) and AA (solid line, red) simulations. The first peak is used to derive the CG bond parameters. The second peak, the next nearest neighbor distance, is controlled by the angle parameters.

The AA RDF is related to the O-C-C-O conformation distributions. The first peak around 2.92 Å is due to the nearest oxygen atoms in the gauche conformation around the C-C bond $-[TG^{\pm}T]_i[TG^{\mp}T]_{i+1}-$, while the second peak at 5.88 Å corresponds to the oxygen atoms in the nearest adjacent ether unit (CH2-O-CH2) in the $-[TG^{\pm}T]_i[TG^{\pm}T]_{i+1}$ conformation. The small peak at 8.24 Å is due to the ether oxygens in the second nearest to the ether element but in a different C-C conformational sequence (TG and TT conformations) [29].

PCL System: Figure 6 compares the intra-molecular Radial Distribution Functions (RDF) between each two core beads C0-C0, N1-N1 and C0-N1 in the CG-PCL_{10} structure and the respective AA structure.

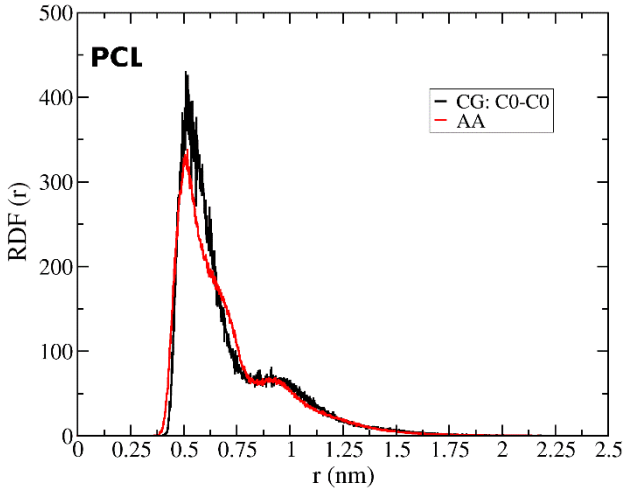
PCL
CG: C0-C0
AA
RDF (r)
r (nm)
0
100
200
300
400
500
0
0.25
0.5
0.75
1
1.25
1.5
1.75
2
2.25
2.5

(a)

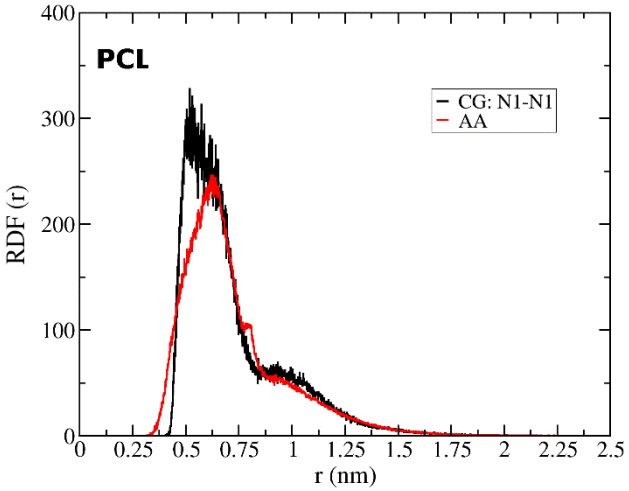
PCL
CG: N1-N1
AA
RDF (r)
r (nm)
0
100
200
300
400
0
0.25
0.5
0.75
1
1.25
1.5
1.75
2
2.25
2.5

(b)

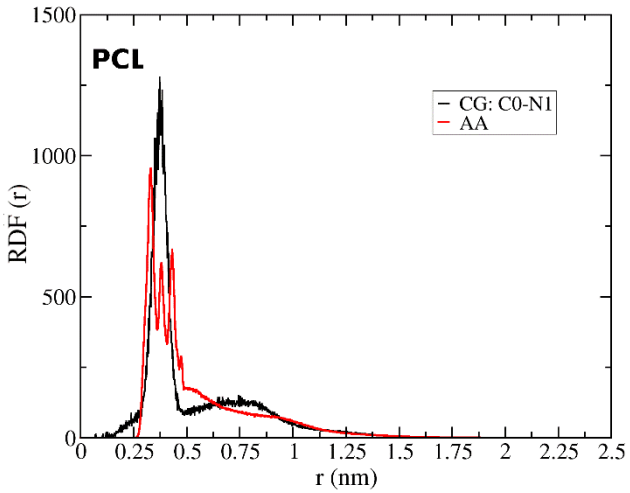

(c)

Figure 6. Radial distribution functions for **(a)** C0-C0 sites, **(b)** N1-N1 sites, and **(c)** C0-N1 sites, from CG (dashed line, black) and AA (solid line, red) simulations. The first peak is used to derive the CG bond parameter. The second peak, the next nearest neighbor distance, is controlled by the angle parameters.

The match between the AA and CG RDFs for each polymer confirms that our CG structures lead to conformations very similar to the AA structures.

3.3.3. Interfacial Properties

For each polymer, we examined both Polymer-Air and Polymer-Water interfaces.

The surface tension across the interface was calculated using the diagonal components of the local pressure tensor [28]:

$$\gamma = \frac{1}{2}\int_0^{L_z} [p_N(z) - p_T(z)]dz \qquad (4)$$

where L_z is the length of the simulation box along the z axis (direction perpendicular to the interface) and $p_N(z) = \frac{p_{xx}(z) + p_{yy}(z)}{2}$ and $p_T(z) = p_{zz}(z)$ are the pressure normal and tangential to the interface.

PEG-Air interface: To calculate the PEG-air interfacial properties, we used a 50 × 50 × 50 Å^3 box of 188 random CG-PEG$_9$ chains (corresponding to PEG400) which was inserted into a 50× 50× 200 Å^3 simulation box. The box was relaxed and equilibrated shortly, followed by a 100 ns production run in the canonical ensemble.

PEG-Water interface: For the PEG-water interfacial properties, we used two unit cells of the CG-PEG crystalline structure with parameters of $a = 7.95$ Å,$b = 25.432$ Å,$c = 19.71$ Å,$\beta = 125.4°$. A second monoclinic cell with same parameters of $a = 7.95$ Å,$b = 25.432$ Å,$c = 19.71$ Å,$\beta = 125.4°$, was filled with 28 MARTINI water beads (the water molecules were added so as to fill the simulation box to a density of approximately 1.02 g/cm^3). The CG-PEG crystalline structure and water film were combined to form a monoclinic cell with parameters $a = 17.00$ Å,$b = 25.432$ Å,$c = 19.71$ Å,$\beta = 125.4°$; each system was subjected to energy minimization to minimize any unphysical bead-bead overlaps.

Two observables were extracted from the simulations of CG-Polymer-Air simulations: interfacial tension and mass density profiles. The calculated surface tension of CG-PEG$_9$-Air is 48.47 mN.m^{-1}, 2% higher than the experimental value of 47.3 mN.m^{-1} for PEG400, validating the NB parameters in our CGq FF. The mass density profile normal to the surface for the CG-PEG$_9$-Air interface is plotted in Figure 7.c. The mass density profile gives a count of the density number of particles as a function of the z coordinates. The density number of CG-PEG$_9$ chains (molecules) in the slab reaches equilibrium at z values between ~65 – 100 Å, the count of molecules falls to zero close to the interfaces with air. The maximum density is 1,340 Kg.m^{-3} and the slab thickness is 20 nm (taking the surface as half the maximum density) (Figure 7.c).

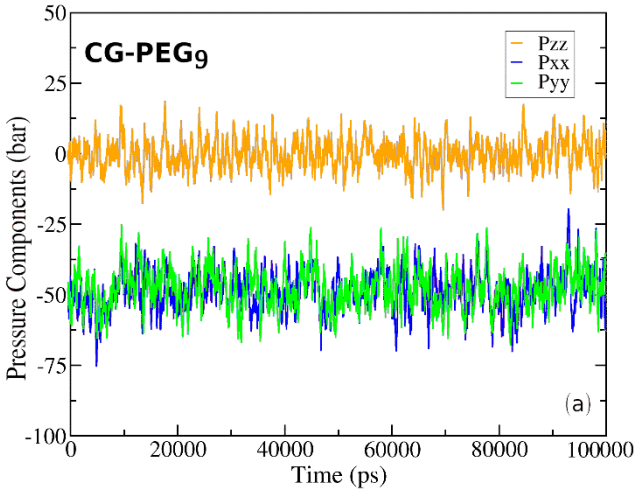

(a)

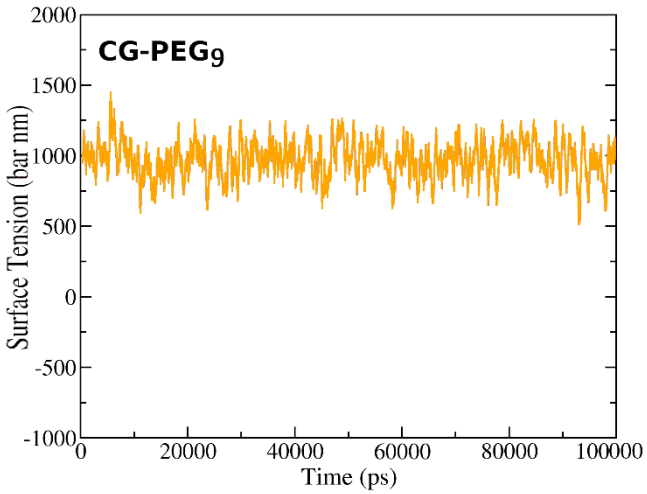

(b)

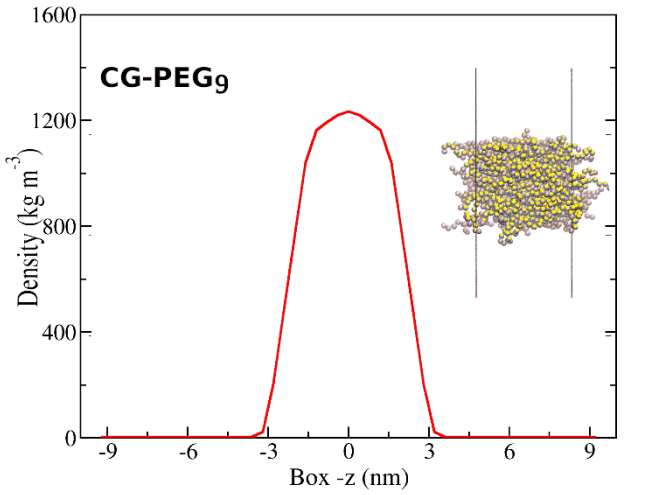

(c)

Figure 7. Properties from 100 ns simulation of CG-PEG$_9$ Vapor Interface **(a)** Pressure components (negative indicates compression) **(b)** Surface tension and **(c)** Mass density profile in z direction (the system is periodic in xy directions).

The interfacial energy for the CG-PEG crystalline structure/water interface was calculated by subtracting the total energy of the minimized combined crystal structure plus the water film from the total energies of each minimized system normalized by the number of molecules, i.e. $COE_{interface} = (TE_{CGPEG-Cryst} + TE_{water-film}) - TE_{combined-sys}$. The calculated molar interfacial cohesive energy per monomer for the CG-PEG crystalline structure at the water interface is 14,640.23 J.mol^{-1}, which is in good agreement with the range of experimental/literature data of

14,000-15,900 J.mol^{-1} (preferred 15,100 J.mol^{-1}) for ethylene glycol monomer, validating the QM derived NB parameters of our CGq FF [30].

PCL-Air interface: to calculate the PCL-Air interfacial properties, 425 random CG-PCL$_{10}$ chains are inserted into a 90× 90× 360 Å^3 simulation box. The box was relaxed and equilibrated, followed by a 100 ns production run in the canonical ensemble.

PCL-Water interface: to calculate the PCL-Water interfacial properties, the unit cell of the relaxed CG-PCL crystalline structure with parameters of $a = 7.144$ Å,$b = 4.799$ Å,$c = 17.168$ Å was combined with another orthorhombic cell with same parameters of $a = 7.144$ Å,$b = 4.799$ Å,$c = 17.168$ Å, filled with 5 MARTINI water beads (the water molecules were added so as to fill the simulation box to a density of approximately 1.02 g/cm^3). The CG-PCL crystalline structure and water film are combined in an orthorhombic cell with parameters $a = 7.144$ Å,$b = 9.598$ Å,$c = 17.168$ Å; each system was subjected to energy minimization to minimize any unphysical bead-bead overlaps.

The calculated surface tension of CG-PCL$_{10}$-Air is 157.811 mN.m^{-1} per interface (Figure 8.b). The mass density profiles normal to the surface for the CG-PCL$_{10}$-Air interface are plotted in Figure 8.c. The density number of CG-PCL$_{10}$ chains (molecules) in the slab reaches equilibrium at z values between ~170 – 200 nm, the count of molecules falls to zero past the interfaces with air, with no CG-PCL$_{10}$ molecules. The maximum density is 2,024.01 Kg.m^{-3} and the slab thickness is 36 nm.

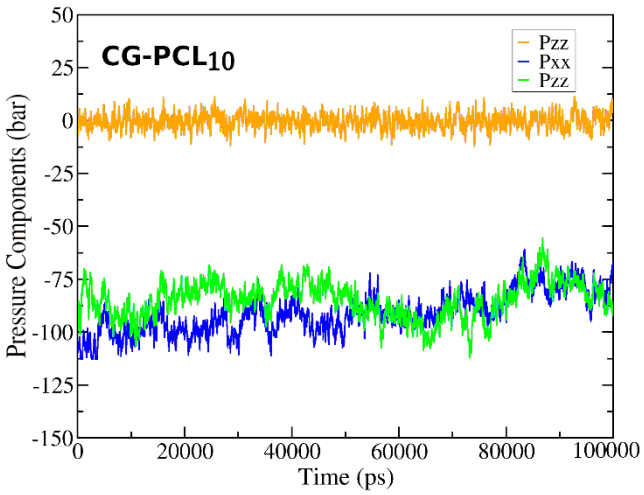

(a)

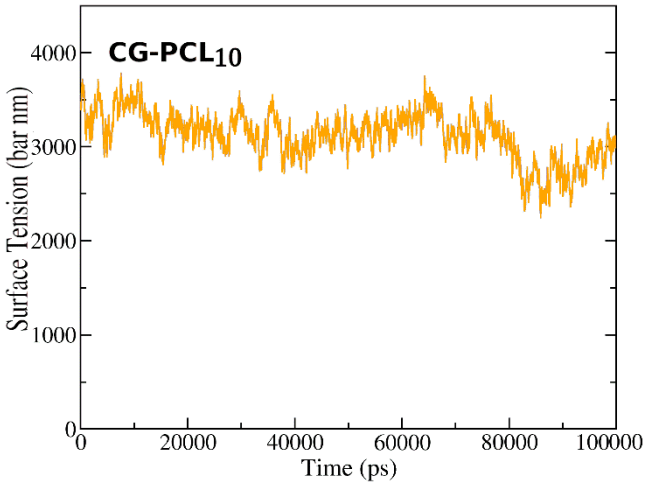

(b)

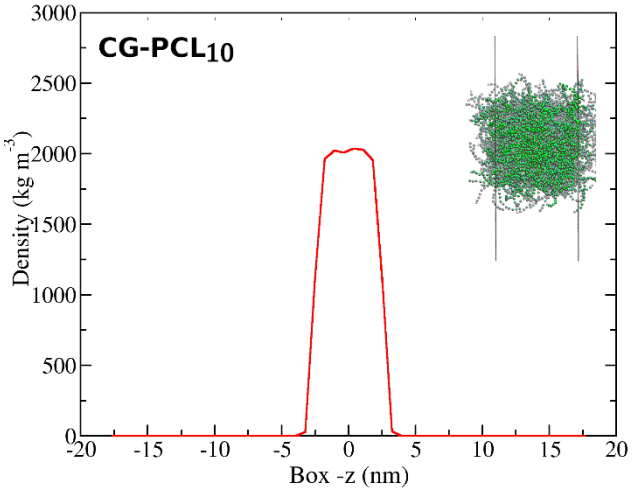

(c)

Figure 8. Properties from 100 ns simulation of CG-PCL$_{10}$ Vapor Interface **(a)** Pressure components (negative indicates compression) **(b)** Surface tension and **(c)** Mass density profile in z direction (the system is periodic in xy directions).

The interfacial cohesive energy for the CG-PCL crystalline structure/water interface was calculated using the same procedures as for PEG. The calculated molar interfacial cohesive energy per chain for the CG-PCL crystalline structure at the water interface is 43,414 J.mol^{-1}, which is in reasonable agreement with the range of experimental/literature data of 37,000-37,350 J.mol^{-1} for PCL, validating the QM derived NB parameters of our CGq FF [30].

3.4. Application: Self-assembly of Amphiphilic PEG-*b*-PCL Diblock Copolymers

The self-assembly of copolymers in solution has been widely investigated both experimentally and theoretically [31]. Block copolymers of PEG-***b***-PCL can self-assemble in aqueous solutions to form micelles with various morphologies and sizes, leading to numerous applications in drug-delivery. In aqueous media, the hydrophobic block (PCL) forms the core while the hydrophilic block (PEG) provides the shell of each micelle. To illustrate the application of our CGq FF, we simulated the self-assembly of 250 isolated CG-MePEG$_{23}$-***b***-PCL$_9$ block copolymers (10,500 beads, corresponding to 123,250 atoms) in water (119,139 water beads, corresponding to 476,552 water molecules) and analyzed the morphology and shape as the micelle formed.

We used the CGq FF (Tables 1 and 2) to characterize the PEG and PCL blocks of the diblock copolymer. To derive the valence parameters for the ester interface linking the two blocks (the ester interface links a Sd1 bead of the PEG block to a N1 bead of the PCL block), we used the AA OPLS/CM1A FF to simulate a single chain of MePEG$_{23}$-***b***-PCL$_9$ in a box of 88.5 Å/side using ~24,600 water molecules, The final AA trajectories were mapped to the CG structure (Figure 9.a). The CG structure was simulated in a box of water with ~6,152 MARTINI water molecules. The final CG parameters for the ester interface is provided in Table 5. The parameterization of the diblock copolymer used the same approach as described in sections 3.2.1.

Table 5. CG Potential Parameters for Ester Part of PEG-*b*-PCL Diblock Copolymer

	Valence Parameters			
	Bond		Angle	
	Simple Harmonic (* 1, 2)		Cosine Harmonic (* 2, 2)	
atom (bead)	K_{bond} $(KJ.mol^{-1}.nm^{-2})$	b_{bond}(Å)	$K_{angle}(KJ.mol^{-1})$	$\theta_0(deg)$
$Sd1-N1$	12,000.000	3.540	-	-
$Sd1-Sd1-N1$	-	-	80.000	125.0
$Sd1-N1-C0$	-	-	40.000	115.0

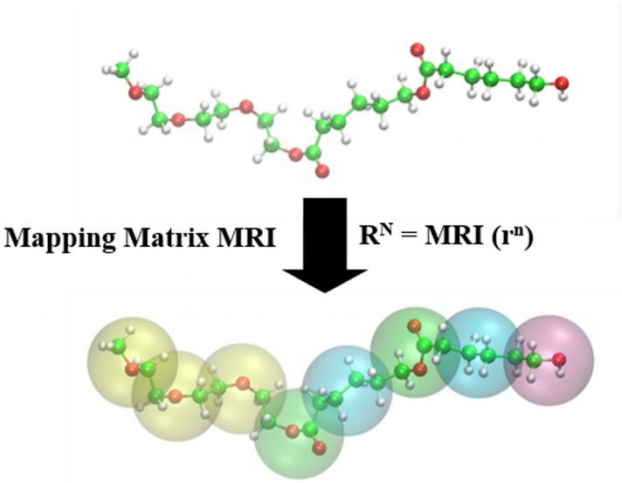

(a)

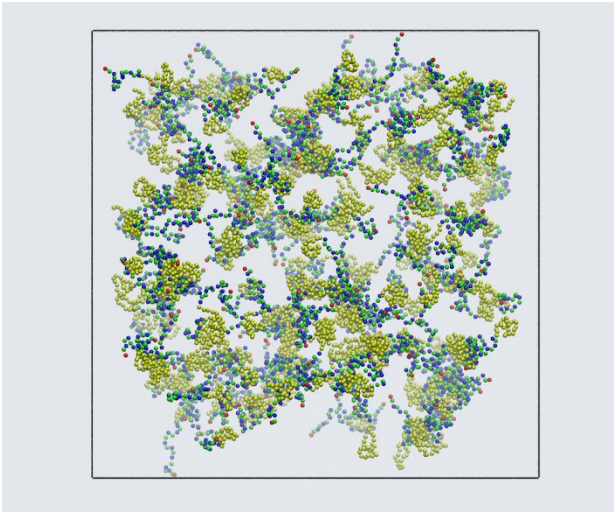

t=1ns

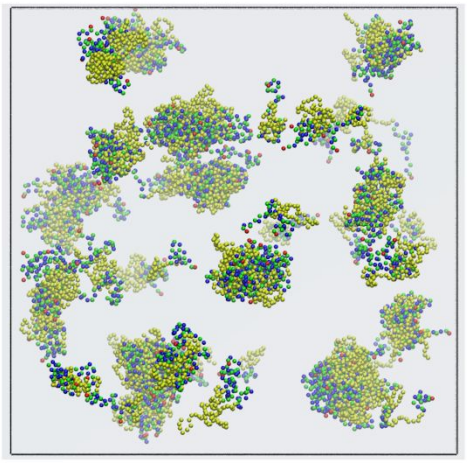

t=20ns

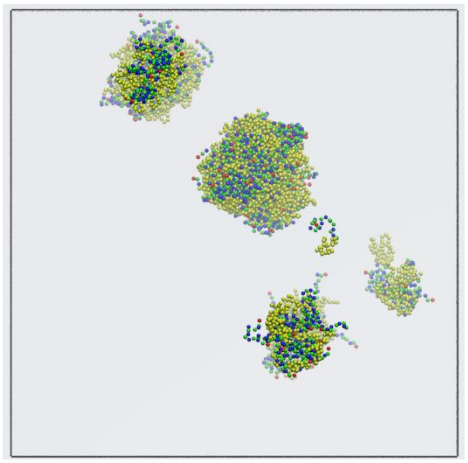

t=200ns

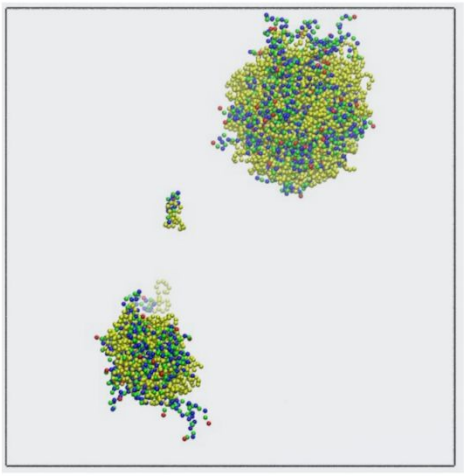

t=500ns

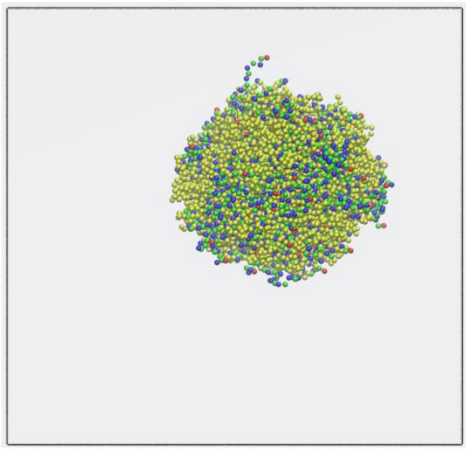

t=1000ns

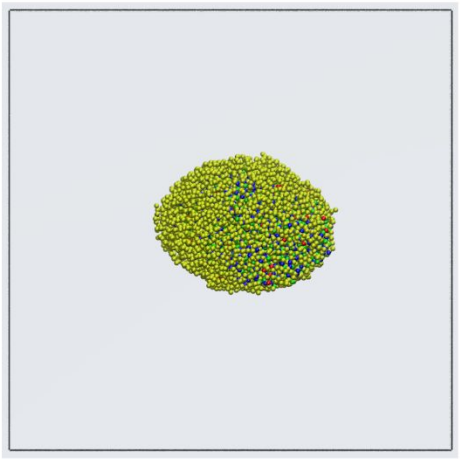

t=2000ns

(b)

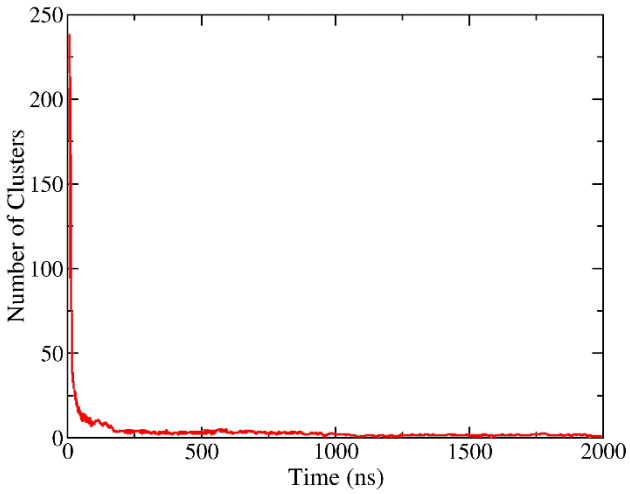

(c)

Figure 9. (a) Illustration for mapping the All-Atom (AA) to the Coarse-Grained (CG) representation of $MePEG_3$-***b***-PCL_2, block copolymer: PEG in yellow (Sd1) and PCL beads: N1-lime, C0-blue and SP2-purple. The ester interface links a Sd1 bead from the PEG block to a N1 bead from a PCL block in the $MePEG_3$-***b***-PCL_2 block copolymer. **(b)** Simulation of micelle formation from self-assembly of $MePEG_{23}$-***b***-PCL_9, block copolymer in water at 310.15K. We started with 250 random single chains (10,500 beads, corresponding to 123,250 atoms) spaced uniformly throughout the simulation box of 250 Å/side. The system was solvated with 119,139 water beads (corresponding to 476,552 water molecules) and simulated over 2μs at 310.15K Color code: PEG in yellow and PCL beads N1-lime, C0-blue and SP2-purple, solvent (MARTINI water) has been removed for clarity. **(c)** Time evolution of the number of clusters of the $MePEG_{23}$-***b***-PCL_9 system in water at 310.15K.

As illustrated in the snapshots of the self-assembly process (Figure 9.b), most chains formed small aggregates within the first 20ns, which then started to combine to form larger aggregates. Finally, they form a spherical micelle, which remains stable until the end of the simulation time, 2 μs. This is illustrated quantitatively in Figure 9.c, showing the time evolution of the cluster numbers in the system over the 2 μs simulation time. We assume that two molecules belong to the same cluster if the distance between the hydrophobic PCL beads is less than or equal to the cutoff of 0.625 nm. This cutoff is based on the position of the first peak in the radial distribution function of the PCL tails.

From Figure 9.b, we see that the micelle forms a core-shell structure with the PCL blocks creating the hydrophobic core and the hydrophilic MePEG blocks forming the shell of the micelle. We analyzed the size and shape of the resulting micelle by computing structural properties such as the radius of gyration Rg, the ratio of principal moments of inertia Ii/Ij, and the asphericity of the

cluster. The results are summarized in Table 6. The averaged ratios of the principle moments of inertia are 0.8 (close to 1), which indicates the quasi-spherical shape of the micelle with an asphericity value of less than 0.005, consistent with experiment [16]. There is no available experimental data reported for the size of this system, however the simulated radius of gyration for the final structure of the micelle is 35.346 Å.

Table 6. Simulated Structural Properties of Micelle formed from Self-assembly of 250 $MePEG_{23}$-*b*-PCL_9 Block Copolymers in Water at 310.15K. Radius of Gyration Rg, Ratio of Principal Moments of Inertia Ii/Ij, and Asphericity.

System	*Rg (Å)*	*I1/I2*	*I1/I3*	*I2/I3*	*Asphericity*
$MePEG_{23}$-***b***-PCL_9	35.346 ± 0.030	0.946 ± 0.010	0.788 ± 0.010	0.822 ± 0.010	0.0033 ± 0.0022

The overall morphology (internal structure) of the final micelle in Figure 10 shows the local density changes of PCL and MePEG blocks with respect to the center of mass (COM) of the micelle; the inset shows the density profile of water with respect to the COM of the micelle. From Figure 10 it is clear that water is excluded from the hydrophobic PCL core.

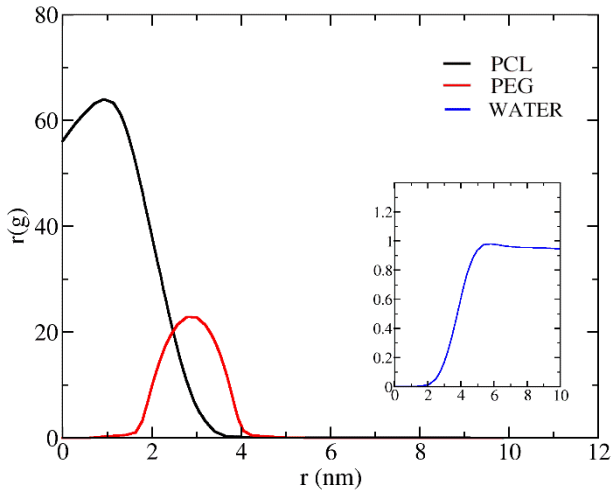

Figure 10. Morphology of the 250 chains $MePEG_{23}$-***b***-PCL_9 micelle after 2 μs at 310.15K. The inset shows the local solvent (MARTINI water) structure.

Conclusion

We report the new CGq FF coarse grain force field for poly(ethylene glycol) (PEG) and poly(ε-caprolactone) (PCL) where the CG NB parameters were obtained to fit the cohesive energy and density from QM on the polymer crystals. We used the functional form for the MARTINI CG FF,

with the CG valence parameters determined to reproduce the bond and angle distributions from All Atom force field simulations.

We validated the accuracy of the NB part of the CGq FF by showing that the interfacial properties of PEG and PCL at the polymer-air interface and the polymer-water interface are in reasonable agreement with experiment (~ 2 % accuracy for PEG and ~ 12 % for PCL).The structural properties (radius of gyration and end to end distance) are also in excellent agreement with atomistic force fields and with experiment.

We illustrated the use of this CGq FF by following the self-assembly of 250 CG-PEG_{23}-***b***-PCL_9 diblock copolymers in aqueous solution on 2 μs timescale, leading to characterization of a quasi-spherical shape micelle in water. We conclude that the CGq FF provides promising means for predicting properties of polymer assemblies for micelles and other complex systems.

Conflict of Interest

We have no conflicts of interest to declare.

Acknowledgments

MSS thanks to Iran University of Science and Technology for the visit of M. S. Sadeghi to Caltech. The Caltech studies were supported by DOE (DE-SC0017710 and DE-AC05-00OR22725).

References

(1) Gartner, T. E.; and Jayaraman, A. Modeling and Simulations of Polymers: A Roadmap. Macromolecules **2019**, 52, 755−786.

(2) Li, Y.; Abberton, B. C.; Kroger, M.; Liu, W. K. Challenges in Multiscale Modeling of Polymer Dynamics. Polymers, **2013**, 5, 751-832.

(3) Monticelli, L.; On Atomistic and Coarse-Grained Models for C60 Fullerene. J. Chem. Theory Comput. **2018**, 8, 1370-1378.

(4) Lopez, C. A.; Rzepiela, A. J.; de Vries, A. H.; Dijkhuizen, L.; Hunenberger, P. H.; Marrink, S. J.; Martini Coarse-Grained Force Field: Extension to Carbohydrates. J. Chem. Theory Comput. **2009**, 5.

(5) Marrink, S. J.; Risselada, H. J.; Yefimov, S.; Tieleman D. P.; de Vries, A. H. The MARTINI Force Field: Coarse Grained Model for Biomolecular Simulations. J. Phys. Chem. B **2007**, 111, 7812-7824.

(6) Lee, H.; de Vries, A. H.; Marrink, S. J.; Pastor, R. W. A Coarse-Grained Model for Polyethylene Oxide and Polyethylene Glycol: Conformation and Hydrodynamics. J. Phys. Chem. B **2009**, 113, 13186–13194.

(7) Lee,H., Larson, R. G. Adsorption of Plasma Proteins onto PEGylated Lipid Bilayers: The Effect of PEG Size and Grafting Density. Biomacromolecules **2016**, 17, 1757−1765.

(8) Rossi, G.; Fuchs, P. F. J.; Barnou, J.; Monticelli, L. A Coarse-Grained MARTINI Model of Polyethylene Glycol and of Polyoxyethylene Alkyl Ether Surfactants. J. Phys. Chem. B **2012**, 116, 14353−14362.

(9) Panizon, E.; Bochiccio, D.; Monticelli, L.; Rossi, G. MARTINI Coarse-Grained Models of Polyethylene and Propylene. J. Phys. Chem B **2015**, 119, 8200-8216.

(10) Nawaz, S.; Carbone, P. Coarse-Graining Poly(ethylene oxide)−Poly(propylene oxide)−Poly(ethylene oxide) (PEO−PPO−PEO) Block Copolymers Using the MARTINI Force Field. J. Phys. Chem. B **2014**, 118, 1648−1659.

(11) Taddese, T., Carbone, P. Effect of Chain Length on the Partition Properties of Poly(ethylene oxide): Comparison between MARTINI Coarse-Grained and Atomistic Models. J. Phys. Chem. B **2017**, 121, 1601−1609.

(12) Grunewald, F., Rossi, G., de Vries, A. H., Marrink, S. J., Monticelli, L. Transferable MARTINI Model of Poly(ethylene Oxide). J. Phys. Chem. B **2018**, 122, 7436−7449.

(13) Choi, E.; Mondal, J.; Yethiraj, A. Coarse-Grained Models for Aqueous Polyethylene Glycol Solutions. J. Phys. Chem. B **2014**, 118, 323−329.

(14) Prasitnok, K.; Wilson, M. R. A coarse-grained model for polyethylene glycol in bulk water and at a water/air interface. Phys. Chem. **2013**, 15, 17093.

(15) Raman, A. S., Vishnyakov, A., Chiew, Y. C. A coarse-grained model for PCL: conformation, self-assembly of MePEG-b-PCL amphiphilic diblock copolymers. Molecular Simulation. **2017**, 43.

(16) Loverde, S. M., Klein, M. L., Discher, D. E. Nanoparticle Shape Improves Delivery: Rational Coarse Grain Molecular Dynamics (rCG-MD) of Taxol in Worm-Like PEG-PCL Micelles. Advanced Materials. **2018**, 1-8.

(17) Shinoda, W., DeVane, R., Klein, M. L. Multi-property fitting and parameterization of a coarse grained model for aqueous surfactants. Molecular Simulation **2007**, 33, 27.

(18) Neyertz, S.; Brown. D.; Thomas, J. O. Molecular dynamics simulation of crystalline poly(ethylene oxide). Journal of Chemical Physics. **1996**, 105, 1668.

(19) Naserifar, S. Oppenheim, J.J., Yang, H., Zhou, T., Zybin, S., Rizk M., Goddard III., W. A. Accurate non-bonded potentials based on periodic quantum mechanics calculations for use in molecular simulations of materials and systems. J. Chem. Phys. **2019**, 151 (15): Art. No. 154111.

(20) G. Kresse and J. Hafner, Ab initio molecular dynamics for liquid metals. Phys. Rev. B, **1993**, 47:558.

(21) G. Kresse and J. Hafner, Ab initio molecular-dynamics simulation of the liquid-metal-amorphous-semiconductor transition in germanium. Phys. Rev. B, **1994**, 49:14251.

(22) G. Kresse and J. Furthmüller. Efficiency of ab-initio total energy calculations for metals and semiconductors using a plane-wave basis set. Comput. Mat. Sci., **1996**, 6:15.

(23) G. Kresse and J. Furthmüller. Efficient iterative schemes for ab initio total-energy calculations using a plane-wave basis set. Phys. Rev. B, **1996**, 54:11169.

(24) CCDC (2017). CSD web interface – intuitive, cross-platform, web-based access to CSD data. Cambridge Crystallographic Data Centre, 12 Union Road, Cambridge, UK.

(25) J. P. Perdew, K. Burke, and M. Ernzerhof. Erratum: Generalized gradient approximation made simple. Phys. Rev. Lett., **1997**, 78:1396.

(26) Bulacu,M., Goga, N., Zhao, W., Rossi, G., Monticelli, L., Periole, X., Tieleman, D. P., Marrink, S. J., Improved Angle Potentials for Coarse-Grained Molecular Dynamics Simulations. J. Chem. Theory Comput. **2013**, 9, 3282−3292.

(27) Kawaguchi, S., Imai, G., Suzuki, J., Miyahara, A., Kitano, T., Ito, K. Aqueous solution properties of oligo-and poly(ethylene oxide) by static light scattering and intrinsic viscosity. Polymer. **1997**, 38, 2885-2891.

(28) Lindhal, E.; Abraham, M. J.; Hess, B.; van der Spoel D. GROMACS 2020 Manual. https://doi.org/10.5281/zendodo.3562512.

(29) Tasaki, K. Poly(oxyethylene)-Water Interactions: A Molecular Dynamics Study. J. Am. Chem. Soc. **1996**, 118, 8459-8469.

(30) @ 2020 polymerdatabase.com

(31) Glover, A. L. Nikles, S. M., Nikles, J. A., Brazel, C. S., Nikles, D. E. Polymer Micelles with Crystalline Cores for Thermally Triggered Release. Langmuir 2012, 28, 10653−10660.

(32) Yuet, P. K.; Blankschtein, D. Molecular Dynamics Simulation Study of Water Surfaces: Comparison of Flexible Water Models. J. Phys. Chem, B **2010**, 114: 13786–13795.

(33) Yeh, I.; Hummer, G.; System-Size Dependence of Diffusion Coefficients and Viscosities from Molecular Dynamics Simulations with Periodic Boundary Conditions. J. Phys. Chem. B **2004**, 108, 15873-15879.

(34) Tanford, C.; Physical Chemistry of Macromolecules; John Wiley & Sons, New York, 1961.

(35) Jorgensen, W. L.; Chandrasekhar, J.; Madura, J. D.; Impey, R. W.; Klein, M. L. Comparison of simple potential functions for simulating liquid water. J. Chem. Phys, **1983**, 79, 926.

(36) Doi, M.; Edwards, S. F. The theory of polymer dynamics; Clarendon Press: Oxford, 1986.

(37) Alexandridis, P.; Hatton, T. A. Poly(ethylene oxide)-poly(propylene oxide)-poly (ethylene oxide) block copolymer surfactants in aqueous solutions and at interfaces: thermodynamics, structure, dynamics, and modeling. Colloids Surfaces A: Physicochem. Eng. Aspects, **1995**, 96, 1-46.

(38) Müeller-Plathe, F.; van Gunsteren, W. F. Molecular Simulation of Polymer-Penetrant Systems Polymer Preprints. Macromolecules, **1994**, 27(21):6040–6045.

(39) Cordeiro, R. M.; Zschunke, F.; Müller-Plathe, F. Transferability of coarse-grained forcefields: The polymer case. J. Chem. Phys. **2008**, 128, 064904, DOI: 10.1063/1.2829409.

(40) Smith, G. D.; Bedrov, D.; and Borodin, O. Conformations and Chains Dimensions of Poly(ethylene oxide) in Aqueous Solutions: A Molecular Dynamics Simulation Study. J. Am. Chem. Soc., **2000**, 122(39):9548–9549.

(41) Underwood, T. R.; Greenwell, H. C. The Water-Alkane Interface at Various NaCl Salt Concentrations: A Molecular Dynamics Study of the Readily Available Force Fields. Scientific RepoRTS, 2018, 8:352, DOI:10.1038/s41598-017-18633-y.

(42) Rose, D.; Rendell, J. Lee, D.; Nag, K.; Booth, V. Molecular dynamics simulations of lung surfactant lipid monolayers. Biophysical Chemistry, **2008**, 138: 67–77.

(43) Henderson, J. A.; Richards, R. W. Organization of Poly(ethylene oxide) Monolayers at the Air-Water Interface. Macromolecules, **1993**, 26: 4591-4600.

(44) Lu, J. R.; Su, T. J.; Thomas, R. K.; Penfold, J.; Richards, R. W. The determination of segment density profiles of polyethylene oxide layers adsorbed at the air-water interfaces. Polymer, **1996**, 37.

(45) Ayranci, E.; Sahin, M. Interactions of polyethylene glycols with water studied by measurements of density and sound velocity. J. Chem. Thermodynamics. **2008**, 40: 1200–1207.

(46) Cranford, S.; Buehler, M. J. Coarse-Graining Parameterization and Multiscale Simulation of Hierarchical Systems. Part I: Theory and Model Formulation. Pages 13-34 of Derosa, P.; and Cagin, T. (eds), Multiscale Modelinh: From Atoms to Devices. Boca Raton, FL, USA: CRC Press.

(47) Arnarez, C.; Uusitalo, J. J.; Masman, M. F.; Ingólfsson, H. I.; de Jong, D. J.; Melo, M. M.; Periole, X.; de Vries, A. H.; Marrink S. J. Dry Martini, a Coarse-Grained Force Field for Lipid Membrane Simulations with Implicit Solvent. J. Chem. Theory Comput. **2015**, 11, 260−275.

(48) Sauer, B. B,; Yu, H. Adsorption kinetics of poly(ethylene oxide) at the air/water interface. Macromolecules **1989**, 22, 786.

(49) Peters, B.L.; Pike, D. Q.; Rubinstein, M.; Grestl, G. S.; Polymers at Liquid/Vapor Interface. SAND. **2018,** 12229J.

(50) Chanda, J.; Bandyopadhyay, S. Molecular Dynamics Study of a Surfactant Monolayer Adsorbed at the Air/Water Interface. J. Chem. Theory Comput. **2005**, 1, 963-971.

(51) Bandyopadhyay, S.; Chanda, J. Monolayer of Monododecyl Diethylene Glycol Surfactants Adsorbed at the Air/Water Interface: A Molecular Dynamics Study. Langmuir. **2003**, 19, 10443-10448.

(52) Bhatt, B.; Newman, J.; Radke, C. J. Molecular Dynamics Simulations of Surface Tensions of Aqueous Electrolytic Solutions. J. Phys. Chem. B. **2004**, 108, 9077-9084.

(53) Jang, S. S.; Lin, Sh. T.; Maiti, P. K.; Blanco, M.; Goddard III, W. A. Molecular Dynamics Study of a Surfactant-Mediated Decane-Water Interface: Effect of Molecular Architecture of Alkyl Benzene Sulfonate. J. Phys. Chem. B. **2004**, 108, 12130-12140.

(54) Jain, A.; Jochum, M.; Peter, C. Molecular Dynamics Simulations of Peptides at the Air−Water Interface: Influencing Factors on Peptide-Templated Mineralization. Langmuir. **2014**, 30, 15486−15495.

(55) Liu, B.; Hoopes, M. I.; Karttunen, M. Molecular Dynamics Simulations of DPPC/CTAB Monolayers at the Air/Water Interface. J. Phys. Chem. B. **2014**, 118, 11723−11737.

(56) Vega, C.; de Miguel, E. Surface tension of the most popular models of water by using the test-area simulation method. The Journal of Chemical Physics. **2007**. 126, 154707.

(57) Graham, J. A.; Essex, J. W.; Khalid, S. PyCGTOOL: Automated Generation of Coarse-Grained Molecular Dynamics Models from Atomistic Trajectories. J. Chem. Inf. Model. **2017**, 57, 650−656.

(58) Buurke, J.; Solubility Parameters: Theory and Application. **1984**, The American Institute for Conservation, Volume Three.

(59) Koenhen, D. M.; Smolders, C. A.; The Determination of Solubility Parameters of Solvents and Polymers by Means of Correlations with Other Physical Quantities. Journal of Applied Polymer Science. **1975**, 19, 1163-1179.

(60) Wang, Y. L.; Lawrence, R. S.; Lu, Z. Y.; Laaksonen, A. Molecular Dynamics Study of Aqueous Solution of Polyethylene Oxide: Critical Test of Force Field Models. Soft Materials. **2013**, 11, 371–383.

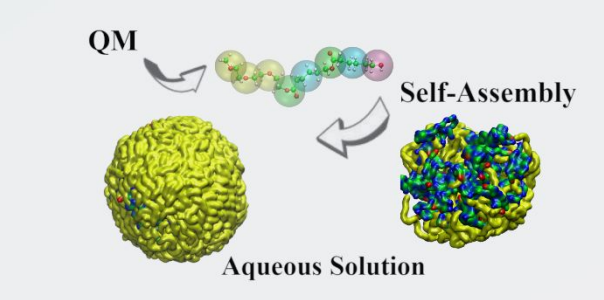

For Table of Contents Use Only. Application of the novel quantum based coarse grained force field (CGq FF) for formation of a micelle from 250 chains of 2000 Dalton CG-MePEG23-b-PCL9 block copolymer in water at 310.15 K.